Journal of Photochemistry and Photobiology A: Chemistry 231 (2012) 19–27

Contents lists available at SciVerse ScienceDirect

Journal of Photochemistry and Photobiology A: Chemistry

journal homepage: www.elsevier.com/locate/jphotochem

Binding interaction between plasma protein bovine serum albumin and flexible charge transfer fluorophore: A spectroscopic study in combination with molecular docking and molecular dynamics simulation

Sankar Jana, Sasanka Dalapati, Shalini Ghosh, Nikhil Guchhait*

Department of Chemistry, University of Calcutta, 92 A. P. C. Road, Kolkata-700009, India

ARTICLE INFO

Article history:
Received 18 August 2011
Received in revised form 25 October 2011
Accepted 4 December 2011
Available online 10 December 2011

Keywords:
BSA
Molecular docking
MD simulation
5-(4-Dimethylamino-phenyl)-penta-2,4-dienenitrile
FRET

ABSTRACT

Binding interaction of plasma protein bovine serum albumin (BSA) with external flexible charge transfer fluorophore 5-(4-dimethylamino-phenyl)-penta-2,4-dienenitrile (DMAPPDN) has been explored at physiological pH (7.4) by steady state absorption, emission, fluorescence anisotropy, Red Edge Excitation Shift (REES), far-UV circular dichroism (CD), time resolved spectral measurements in combination with molecular docking and molecular dynamics (MD) simulation studies. Chemical denaturation of the protein bound probe by guanidine hydrochloride (GdnHCl) has also been tracked using the spectral response of DMAPPDN. Interaction of the probe with BSA is reflected by the massive blue shift of the fluorophore emission maxima (78 nm) with the enhancement of fluorescence intensity due to change of hydrophobic micro-environment of the probe compared to a little change in protein secondary structure. Benesi–Hildebrand plot reveals spontaneous formation of 1:1 BSA–DMAPPDN complex with binding constant $8.821 \pm 0.01 \times 10^3\ M^{-1}$ and binding free energy change -5.359 kcal mol^{-1}. Molecular docking study supports the binding of probe in the hydrophobic cavity of sub domain IIA of BSA. The distance for energy transfer from tryptophan of BSA to DMAPPDN measured from fluorescence resonance energy transfer (FRET) results is in good agreement with results of molecular docking study. MD simulation predicts greater stability of BSA–DMAPPDN complex compared to the free protein.

1. Introduction

Serum albumins are major transport proteins [1,2] found in the blood plasma and are capable of binding, transporting and delivering an extraordinarily diverse range of endogenous and exogenous compounds like fatty acids, nutrients, steroids, certain metal ions, hormones and a variety of therapeutic drugs [3–5] in the bloodstream to their target organs [6]. Although a large volume of research work is already established in diverse fields with BSA as a model protein, but till date, there exists an intriguing mystery regarding the various types of hydrophobic and hydrophilic interactions within the protein interior in the presence and absence of small molecules like drugs and/or fluorescent probes, since, the exact crystal structure of BSA is still unknown. The crystal structure of human serum albumin (HSA) is however well established. The pair wise sequence alignment has only one gap over all the residues of the BSA sequence with 75% identity and 87% similarity shared between human and bovine sequences [7]. The primary structure of BSA is a sequence of 583 amino acid residues and the secondary structure contains 67% alpha helix with six turns and 17 disulphide linkages [4,8–10]. The tertiary structure is formed by three homologous domains I→III, each of which is divided into two sub domains A and B [4,11]. Two tryptophan residues Trp-134 and Trp-213 are present in BSA in the IB and IIA sub domains, respectively [12–14]. This protein also contains two principal drug binding sites, site-I and site-II. Site-I is situated in the hydrophobic core of sub domain IIA which is capable of binding mostly with neutral, bulky heterocyclic compounds by strong hydrophobic interactions, whereas site-II is in the IIIA sub domain and binds many aromatic carboxylic acids by dipole–dipole, van der Waals and hydrogen bonding interactions [15]. The structural aspects of serum albumins and their properties and interactions with other materials have been explored by several groups [16,17] using NMR, dynamic light scattering, differential scanning calorimetry, circular dichroism and other techniques. In the last few years, in the field of photochemistry and photobiology, the intramolecular charge transfer (ICT) fluorescent molecules were used as fluorescence probes for the study of bio-mimetic micro-heterogeneous environments [18], and for sensing the local polarity of the microenvironment around their binding sites on biologically relevant systems like proteins [16]. Fluorescent probe spectroscopy is also rapidly gaining importance as a non-invasive efficient technique compared to the complex and

* Corresponding author. Tel.: +91 033 2350 8386; fax: +91 33 2351 9755.
E-mail address: nguchhait@yahoo.com (N. Guchhait).

1010-6030/$ – see front matter © 2011 Elsevier B.V. All rights reserved.
doi:10.1016/j.jphotochem.2011.12.002

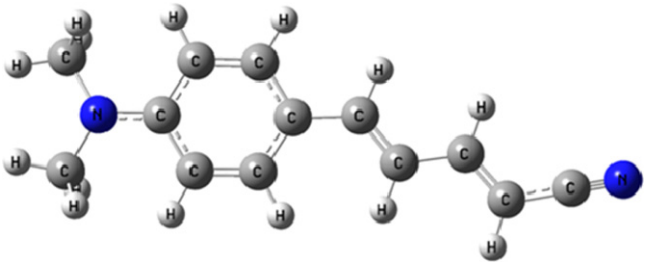

Scheme 1. Optimized structure of 5-(4-dimethylamino-phenyl)-penta-2,4-dienenitrile (DMAPPDN) at HF/6-31+G(*d*,*p*) level. The final structure was generated by Gauss View software.

expensive techniques such as X-ray or NMR analysis for studying the chemical unfolding of these proteins induced by agents like guanidine hydrochloride, urea and surfactants. In recent times, the studies of structural and dynamical aspects of such biological systems using new synthetic extrinsic polarity sensitive fluorescent probes are gaining extra momentum especially when the experimental findings corroborate the results of molecular docking [19–21] and molecular dynamics simulation [19,22,23].

In this work, we report the use of a specially designed polarity sensitive intramolecular charge transfer molecule 5-(4-dimethylamino-phenyl)-penta-2,4-dienenitrile (DMAPPDN) (Scheme 1) as an extrinsic fluorescent probe for studying BSA microenvironment [24]. Monitoring denaturation with guanidine hydrochloride was also attempted using the spectral response of the probe. Steady state absorption, emission, fluorescence anisotropy, REES, CD and time resolved spectral measurements have been used in this context. Molecular level interactions, conformational changes of protein BSA after binding with the probe and flexibility at the binding sites have been explored by spectroscopic measurement hand in hand with molecular docking and molecular dynamics simulations. This work is very unique because our designed molecule, DMAPPDN can probe protein structure and dynamics easily with only absorption and emission spectral responses and molecular modeling without involving any complex X-ray or NMR analysis. Also this study makes way for the probable application of this specially designed molecule DMAPPDN as an effective fluorescent probe for spectroscopic investigation of such other biological systems.

2. Experimental methods

2.1. Reagents

The synthetic scheme, procedure and purification of DMAPPDN have been described in our earlier publication [24]. GdnHCl and BSA were purchased from SRL India and used as received. 10^{-3} M DMAPPDN, 10^{-6} M BSA and 9 M GdnHCl solutions were prepared in 0.01 M Tris–HCl buffer solution corrected to pH = 7.4 by the addition of 1:1 HCl and used as stock solutions. Triply distilled water was used for preparing all solutions. The purity of all solvents in the studied wavelength range was checked before the preparation of solutions. All solutions of DMAPPDN and BSA were prepared at the desired concentrations and equilibrated for 6–7 h before spectral measurements.

2.2. Measurement of steady state absorption and emission and CD spectroscopy

All steady-state absorption spectra were recorded on a Hitachi UV/VIS U-3501 spectrophotometer. The emission spectra and fluorescence anisotropy were recorded on a Perkin Elmer LS-55 fluorescence spectrophotometer after proper background corrections with individual solvents. Concentration of the probe was kept at $\sim 10^{-6}$ M for all measurements to ensure no occurrence of self aggregation or self quenching and also to maintain probe concentrations at a much lower value than the protein. The alterations in the secondary structure of the protein in the presence of probe were studied by far UV circular dichroism measured by a Jasco Corporation, J-815 CD spectrophotometer using a quartz cuvette of path length 0.1 cm at 1 nm data pitch intervals. All CD spectra were recorded in the wavelength range 190–250 nm. The spectrophotometer was sufficiently purged with 99.9% nitrogen before measurements. The spectra were collected at a scan speed of 50 nm/min with response time of 1 s at 298 K temperature. Each spectrum was baseline corrected with Tris–HCl buffer and the final plot was taken as an average of four accumulated plots.

2.3. Time resolved spectral measurement

Fluorescence lifetimes were determined from time-resolved intensity decay by the method of time correlated single-photon counting (TCSPC) using a picosecond diode laser (IBH, U.K. nanoLED) [25] as the light source at 370 nm. The typical instrumental response of this excitation source is ~40 ps. A Hamamatsu MCP photomultiplier tube (5000U-09) collected the emission at a magic angle polarization. The TCSPC setup consists of an Ortec 9327 CFD and a Tennelec TC 863TAC. Data collection was done with a PCA3 card (Oxford). An IBM DAS6 software was used to deconvolute the fluorescence decays.

2.4. Molecular docking study

Molecular docking was performed to obtain the protein-ligand binding energy and to identify the potential ligand binding sites. The docking experiments were performed with the help of AutoDock4.2 [26] and AutoDock Tools (ADT) software using the Lamarkian Genetic Algorithm (LGA) based on the adaptive local method search. The energy based Autodock scoring function includes terms accounting for short range van der Waals and electrostatic interactions, loss of entropy upon ligand binding, hydrogen bonding and solvation. For the recognization of the binding sites in BSA, docking was carried out with setting of grid box size 126 Å × 96 Å × 126 Å along *x*, *y*, *z* axes covering whole protein with a grid spacing 0.508 Å [19] after assigning the protein and probe with Kollman charges. The grid center was set at 0.026, 0.108, and 0.114 Å. At first, AutoGrid was run to generate the grid map of various atoms of the ligand and receptor. After the completion of grid map, ligand flexible docking simulations were performed with 200 runs and 2.5×10^6 energy evaluations, 27,000 numbers of generations, 50 GA population and root mean square cluster tolerance 2.0 Å [23] per run. Among 200 runs 10 minimum energy conformers were chosen according to ranking and scoring [20,23]. Finally the lowest energy conformation was used for docking analysis.

2.5. MD simulation protocol

The MD simulations were carried out using NAMD 2.6 software [27] and CHARMM22 force field and parameters [28]. Preparation of protein and probe structures has been mentioned in the supplementary data. Protein structure file (psf) for both the BSA and probe of our interest were prepared by Vega ZZ 2.4 (http://www.vegazz.net) [29] software. At first, the protein was neutralized with 17 Na^+ ions after being immersed in TIP3P water box containing 25,372 water molecules with box dimension of 95 Å × 86 Å × 98 Å by using VMD 1.8.7. software [30]. We have prepared two water boxes, first one containing water, protein and Na^+ ions with total numbers of 85,251 atoms and the other box with water, protein, Na^+ ions and the probe with 85,280 atoms.

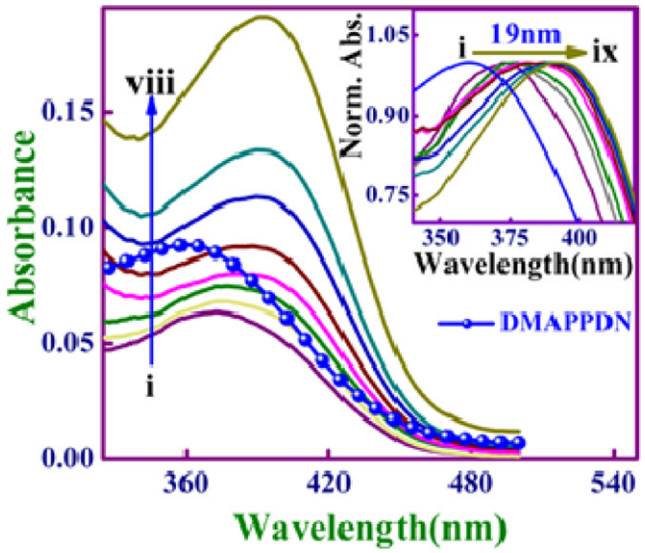

Fig. 1. Absorption spectra of DMAPPDN with increasing concentration of BSA. (i→viii) 10, 20, 30, 50, 60, 70, 80, and 90 μM BSA. Inset shows the normalized absorption spectra (i→ix) 0, 10, 20, 30, 50, 60, 70, 80, and 90 μM BSA.

In the second box the probe was placed with in the sub domain IIA hydrophobic zone of BSA as we have observed the binding nature of protein and probe from the molecular docking study [23]. The MD simulation of these two systems was performed using four stages. In the first stage, 5000 steps energy minimization were carried out at 0 K using a harmonic constraints 500 kcal mol^{-1} $Å^{-2}$ on alpha carbon atom of protein and probe. Then entire system was energy minimized for 5000 steps without any harmonic restrain. In the next stage of the equilibration protocol, the systems were heated from 0 K to 310 K increasing by 5 K temperature every 2000 steps of a 313 ps dynamics with restraints on the solute. In this stage, we have used Langevin thermostat to maintain temperature. The final steps were 7 ns NPT dynamics using the Langevin piston pressure control at 310 K and 1.01325 bar. Periodic boundary conditions and the Particle-mesh Ewald method [31] were applied for a complete electrostatics calculation. Also the Langevin damping coefficient and piston decay were set as 5 ps^{-1} and 50 fs, respectively. The temperature was maintained at 310 K using Langevin dynamics. Non-bonded interactions were calculated by applying a 10 Å cut-off, with a switching function at 8 Å. The non-bonded list generation was stopped at 11.5 Å [22]. Simulation was carried out with an integration time step of 2 fs using SETTLE algorithm, while keeping all bonds to hydrogen atoms rigid. The trajectory was stored every 2 ps and further analyzed with the VMD programme and tcl script for root mean square deviations (RMSD) [22,32], root mean square fluctuations (RMSF) [32] and radius of gyration (R_g) [23].

3. Results and discussion

3.1. Absorption spectral measurement

The absorption spectra of the probe DMAPPDN in nonpolar, polar protic and polar aprotic solvents were reported in our previous publication [24]. As shown in Fig. 1, the absorption band of DMAPPDN in water is shifted to red from ~372 nm to ~391 nm by gradual increase in the concentration of added BSA from 0 to 90 μM. The new red shifted absorption band at 391 nm originates from the BSA–DMAPPDN complex. This red shift may be due to the stabilization of the complex compared to the free probe in water or movement of the probe from aqueous media to hydrophobic media of the protein interior [16,18,33]. The red shift of 19 nm is

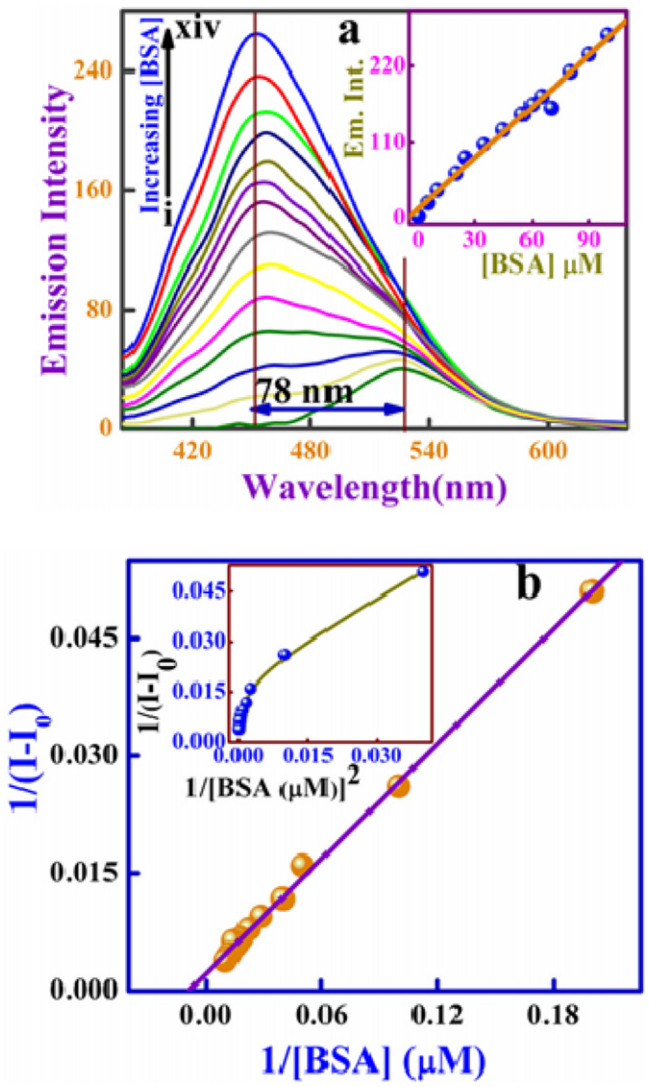

Fig. 2. (a) Emission spectra of DMAPPDN (λ_{ex} = 372 nm) with increasing concentration of BSA. (i→xiv) 0, 5, 10, 20, 25, 35, 45, 55, 60, 65, 70, 80, 90, and 100 μM BSA. Inset: plot of emission intensity vs BSA concentration. (b) B–H plot for 1:1 complexation of DMAPPDN with BSA. Inset: nonlinear B–H plot for 1:2 complexation of DMAPPDN and BSA.

better represented by the normalized absorption spectra as shown in inset of Fig. 1.

3.2. Effect of BSA on DMAPPDN fluorescence

We have earlier reported dual fluorescence from DMAPPDN in polar solvents due to excited state intra-molecular charge transfer from the donor amine group to the acceptor nitrile group [24]. The high energy band at ~425 nm was assigned to emission from the locally excited (LE) state and the low energy band at ~530 nm to the CT state. To follow the probe–protein interaction, the emission spectra of the probe were recorded at a fixed concentration of DMAPPDN with progressively increasing the concentration of BSA. The emission maximum of the probe undergoes a large blue-shift from ~530 nm in 0.01 M tris buffer to 452 nm in 90 μM BSA (78 nm) with a simultaneous increase in fluorescence intensity (6.5 times) as shown in Fig. 2a. This blue-shift of the polarity sensitive CT maxima points towards a lowering of polarity of surrounding environment of the probe on binding to BSA. This is expected as the probe on binding with protein moves to a less polar hydrophobic proteinous environment from the highly polar aqueous buffer.

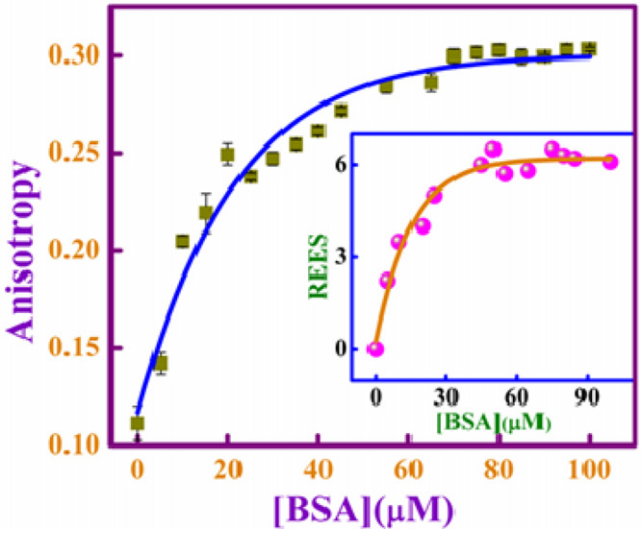

Fig. 3. Plot of anisotropy vs concentration of BSA at 298 K temperature. The data points are mean of five independent measurements, the standard errors were between 1.0×10^{-3} and 8.9×10^{-3} for all data points. Inset: Plot of REES vs concentration of BSA at 298 K temperature for the interaction of BSA with DMAPPDN.

Usually movement of the probe to a more hydrophobic environment deactivates the non-radiative decay paths that operate in water via hydrogen bonds. This is then marked by the simultaneous increase in intensity of the intramolecular charge transfer emission band [16,18,33]. The increase in emission intensity as a function of protein concentration is better represented by the inset of Fig. 2a.

3.3. Protein–probe complexation study

To gain a better insight into the binding of DMAPPDN with BSA we have constructed the well known Benesi–Hildebrand (B–H) plot [34] for 1:1 association and found it to be linear through the entire BSA concentration range studied. The linearity ($R = 0.9988$) of the plot (Fig. 2b) throughout the entire range of the data is a proof of 1:1 complexation between the protein and the probe. From this plot the values for the association or binding constant and the free energy change accompanying the binding process were calculated to be $8.821 \pm 0.01 \times 10^3\ M^{-1}$ and $-5.359\ kcal\ mol^{-1}$, respectively (Table 1). This observation indicates [16,33] comparatively strong binding of DMAPPDN to the model protein. To confirm our assumption, we have also constructed the B–H plot for 1:2 complexation as shown in inset of Fig. 2b. The nonlinear B–H plot in this case also supports that the BSA–DMAPPDN complexation occurs only through 1:1 stoichiometry.

3.4. Study of steady state fluorescence anisotropy

The changes of emission profile of DMAPPDN upon binding with BSA suggest its movement from the free aqueous environment to the proteinous environment which is also mirrored in the changes in fluorescence anisotropy. Increasingly rigid environments restrict free motion of the probe and produce higher values of anisotropy [18,33,35]. So anisotropy measurements can be exploited to gain more information about the rigidity of the environment surrounding a fluorescent probe and the extent to which this rigid environment actually impedes the motional dynamics of the former. The protein interior being more rigid than the free water environment, and hence the BSA bound probe must experience a restriction of its rotational motion. As seen in Fig. 3, a sharp rise of anisotropy till 20 μM BSA is observed and then the anisotropy value increases smoothly till 55 μM BSA to a value of 0.284. The maximum anisotropy value of 0.299 was recorded at and after 70 μM BSA environment which is quite high and suggests a good extent of association between DMAPPDN and BSA. The leveling off of the anisotropy values from around and after 70 μM BSA is again consistent with other related similar systems [16,33,35,36].

3.5. Wavelength sensitive fluorescence measurement

Red Edge Excitation Shift [35] is a well known phenomenon which provides a more vivid picture of the surrounding atmosphere of a polar probe while emitting from the excited state. This technique comes in handy to monitor directly the environment and dynamics around a fluorophore in a complex biological system. An increase in REES values with increasing concentration of protein indicates greater restriction on the mobility of the solvent molecules surrounding the probe molecule bound within the hydrophobic cavity of the protein. Therefore to establish the environmental rigidity and the solvent relaxation dynamics around the BSA bound probe, we have measured the REES of DMAPPDN emission maximum [37,38] as a function of BSA concentration. As shown in inset of Fig. 3, with a 10 nm red-shift in excitation wavelength, REES values increase as a function of BSA concentration and reached a maximum value of 6 nm for 45 μM BSA after which it remains almost unchanged even up to 100 μM BSA. This is a clear evidence that after interaction, the probe molecules move to the more restricted protein interior which explains the observed increase in the red edge shift [16].

3.6. Time resolved measurement

Fluorescence lifetimes were measured to further investigate the excited state behavior and microenvironment surrounding the excited probe [13,39,40]. The time resolved fluorescence measurements of an intrinsic fluorophore like tryptophan in BSA are complex in nature. Therefore, to investigate the micro environment around the probe, we have measured the fluorescence life time of the extrinsic fluorophore DMAPPDN. The fluorescence decay curve for such probe and protein binding process in heterogeneous media are multiexponential in nature [39,40], but in our system the fluorescence decay curves were fitted by bi and tri-exponential function with acceptable χ^2 values (Table 2). As seen in Table 2, the results show that the average fluorescence life time of DMAPPDN increases with change in environment from aqueous tris buffer ($\langle\tau\rangle = 0.248$ ns) to protein medium ($\langle\tau\rangle = 3.4$ ns). This increment in average lifetime again supports the movement of the probe to the protein interior, where the nonradiative decay channels are not operative like that in the aqueous media [39,41,42]. The two exponential decay components for DMAPPDN may be due to the presence of the two excited state species as obtained for many such intramolecular charge transfer probes [43–45]. One may be due to the local emission and other is due charge transfer state [43]. On the other hand, the origin of this triple exponential decay is not very clear. But, in analogy to other such studies, it can be said that different components may arise due to binding of the probe to different binding sites of the protein [33,35].

3.7. Chemical denaturation of BSA by GdnHCl

Denaturation of protein is a complicated process which occurs through diverse array of mechanism [46,47]. GdnHCl is a well known chemical denaturing agent which disrupts the tertiary structure of proteins [36]. Here we study the chemical denaturation of BSA by GdnHCl using steady state emission spectra, anisotropy and REES of the extrinsic fluorophore DMAPPDN bound to BSA. As shown in Fig. 4a, with an increase in the concentration of GdnHCl (0–4 M) added to 15 μM BSA solution, the intensity of the emission

Table 1
Experimental and theoretical data obtained from complexation of BSA and DMAPPDN.

	$-\Delta G$ (kcal mol^{-1})	K ($\times 10^{-3}$ M^{-1})	r (nm)
Experimental	5.359	8.821 ± 0.01	3.24 ± 0.02
Theoretical	4.54	2.20 ± 0.02	1.65 ± 0.01 (Trp-213) 3.33 ± 0.02 (Trp-134)

Where ΔG, K and r are Gibbs' free energy change due to BSA and DMAPPDN complexation, stability constant of the complex and average distance of DMAPPDN from Tryptophan, respectively.

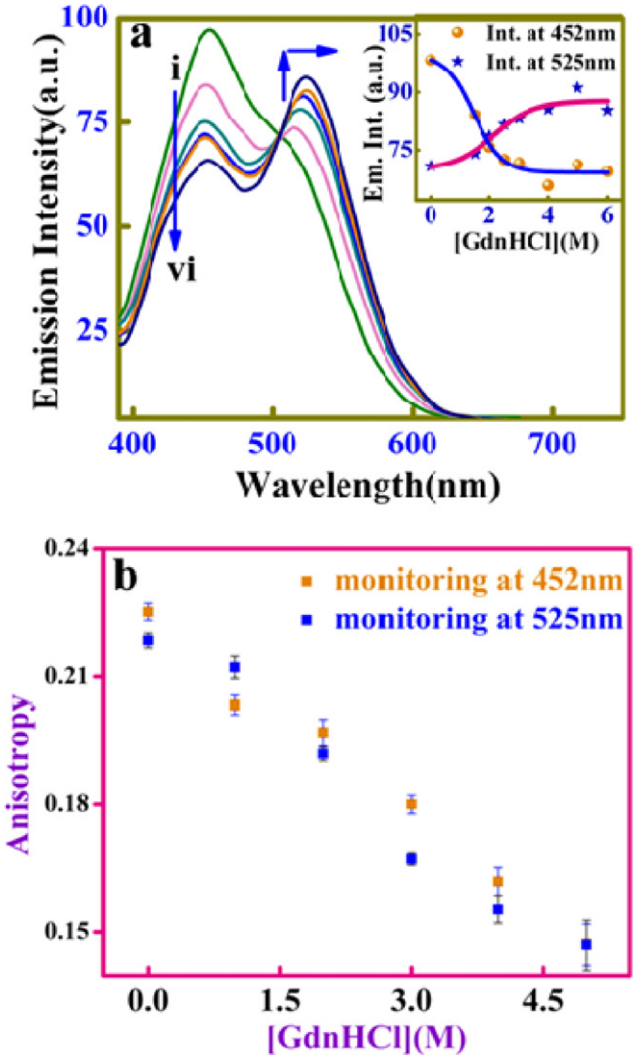

Fig. 4. (a) The emission spectra of BSA bound DMAPPDN (λ_{ex} = 372 nm) as a function of GdnHCl concentration, (i→vi) 0, 1.5, 2, 2.5, 3, and 4 M GdnHCl. Inset shows plot of emission intensity of two emission band at 452 and 525 nm vs concentration of GdnHCl (M). (b) Plot of anisotropy vs concentrations of GdnHCl (M) for both high (452 nm) and low (525 nm) energy band at 298 K temperature. The data points here are the mean of five independent measurements, the standard errors were between 1.4×10^{-3} and 5.8×10^{-3} for all data points.

band of BSA-DMAPPDN complex at 452 nm decreases with a concomitant generation of a new band at 525 nm. With further increase in GdnHCl concentration till up to 8 M further spectral change was not observed. The decrease in emission intensity of the LE band with increasing GdnHCl is mainly due to denaturation of BSA and

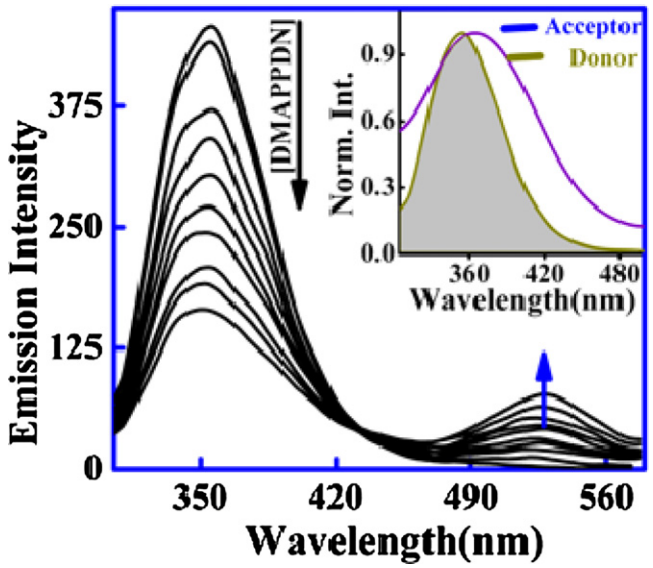

Fig. 5. The occurrence of FRET with increasing concentration of DMAPPDN (arrow indicates increasing probe concentrations). Inset shows the shaded area is the common region between emission spectra of donor and absorption spectra of acceptor.

movement of the probe from hydrophobic protein interior to the polar aqueous media. It is to be pointed out here that the probe shows its emission at 525 nm in pure water. Inset of Fig. 4a shows the plot of emission intensity as a function of GdnHCl concentration, where both the decrease of emission intensity at 452 nm and increase at 525 nm respectively are found to be sigmoidal in nature. Again to establish the denaturation process we also measured the anisotropy values by monitoring at the emission maxima positions and are shown in Fig. 4b. From the figure it is clear that for both the cases initial anisotropy value of 0.225 for the complex formed by 15 μM BSA, decreases to ~0.147 with the addition of 5 M GdnHCl. This supports the inference that the probe moves from the more restricted hydrophobic medium to the less restricted aqueous zone on denaturation and unfolding of the protein.

3.8. Fluorescence resonance energy transfer

In recent times, among various experimental methods for calculating the donor acceptor distances, fluorescence resonance energy transfer is one of the best methods often described as a molecular ruler. The efficiency of FRET depends on the overlap between emission spectra of the donor and absorption spectra of the acceptor as also on the proper relative orientation of the donor and acceptor transmission dipoles. Maintenance of optimum distance between donor and acceptor is also vital for FRET process. Inset of Fig. 5 shows a large overlap region between the tryptophan emission

Table 2
Time resolved spectral data of DMAPPDN in Tris buffer and BSA.

Medium	τ_1 (ns)	τ_2 (ns)	τ_3 (ns)	a_1	a_2	a_3	χ^2	$\langle\tau\rangle$ (ns)
Tris buffer	0.062	3.537	–	0.998	0.001	–	1.10	0.248
70 μM BSA	1.193	0.063	6.840	0.039	0.949	0.013	1.29	3.400

band of BSA and the absorption band of probe DMAPPDN which makes the possibility of efficient FRET [12,16] from tryptophan to the bound probe. Fig. 5 shows the actual occurrence of FRET between tryptophan of BSA and the bound probe. The tryptophan emission at 350 nm obtained on exciting the protein solution at the tryptophan absorption maxima of 295 nm, was found to be gradually quenched with increasing concentration of the probe while simultaneously a new band exactly at the position of the observed emission maxima of DMAPPDN appeared and gained intensity. It is noteworthy that at 295 nm there is no observable absorption of DMAPPDN and hence it is evident that the appearance of the emission maxima of the probe as explained above can only take place via FRET from tryptophan to the probe. The efficiency of energy transfer (E) from the donor tryptophan of BSA to the acceptor probe was calculated to be 63.9%. Using the calculated value of $J = 1.4976 \times 10^{-14}\,\mathrm{L\,mol^{-1}\,cm^3}$ and the literature values for $\kappa^2 = 2/3$, $n = 1.36$ and $\Phi = 0.15$, the R_0 and r values were found to be 2.73 ± 0.01 nm and 3.24 ± 0.02 nm, respectively (where J, κ^2, n, Φ, R_0, r are the overlap integral between donor emission and acceptor absorption, spatial orientation factor, refractive index of the medium, fluorescence quantum yield of the donor, critical distance at which the extent of energy transfer is 50% and distance between donor and acceptor, respectively). The FRET measurement thus supports the fact that the probe is very near to the tryptophan of BSA having tight binding characteristics.

3.9. Molecular docking analysis

Among the various conformers of docking results, only 10 conformers were chosen on the basis of the free energy of binding and score ranking [20,23]. The minimum binding energy conformer is shown in Fig. 6a and all the data related to complexation and binding processes are reported in the Table S1 (supplementary data). In BSA, there are two principal drug binding sites which are located in the hydrophobic cavities of sub domains IIA and IIIA [12,13,15]. The minimum energy conformer showed that the ligand binds within the hydrophobic pocket of sub domain IIA. As shown in Fig. 6b, the probe molecule is surrounded by the hydrophobic side chains and positively charge hydrophobic residues, such as Ala-212, Val-215, Phe-227, Val-234, Leu-326, Gly-327, Leu-346 and Arg-208. Therefore it can be concluded that the interaction between the DMAPPDN and BSA is mainly hydrophobic in nature. Also there are considerable number of hydrogen bonding and electrostatic interactions due to the presence of several ionic and polar groups like Lys-211, Asp-323, Glu-353 and Thr-231, Thr-235 near the probe molecule. Considering the distance between donor and acceptor atoms from 2.6 to 3.5 Å [20,23], we have found one hydrogen bond between nitrile N atom of DMAPPDN and the adjacent O atom of the hydroxyl group of Thr-235 (2.85 Å) (Fig. 6b). Hydrogen bonding supports decrease in hydrophilicity instead of increasing hydrophobicity within the BSA–DMAPPDN complex [20,23]. From the docking simulation the observed free energy change of binding (ΔG) for the complex BSA–DMAPPDN is found to be $-4.54\,\mathrm{kcal\,mol^{-1}}$, which is less comparable to our experimental free energy of binding ($-5.359\,\mathrm{kcal\,mol^{-1}}$) obtained from complexation study by Benesi–Hildebrand plots [34]. This difference between experimental and theoretical results may be due to exclusion of solvent in docking simulations or rigidity of the receptor other than tryptophan. On the other hand, the distance between tryptophan and the bound probe obtained from FRET calculation (3.24 ± 0.01 nm) is also comparable to the distances obtained from docking simulation where distances of the probe are found to be 1.65 ± 0.01 nm and 3.33 ± 0.02 nm from Trp-213 and Trp-134, respectively (Fig. 7a). For comparison, the binding free energy data, stability constant and distance between tryptophan and the probe obtained from theoretical and experimental results are given in

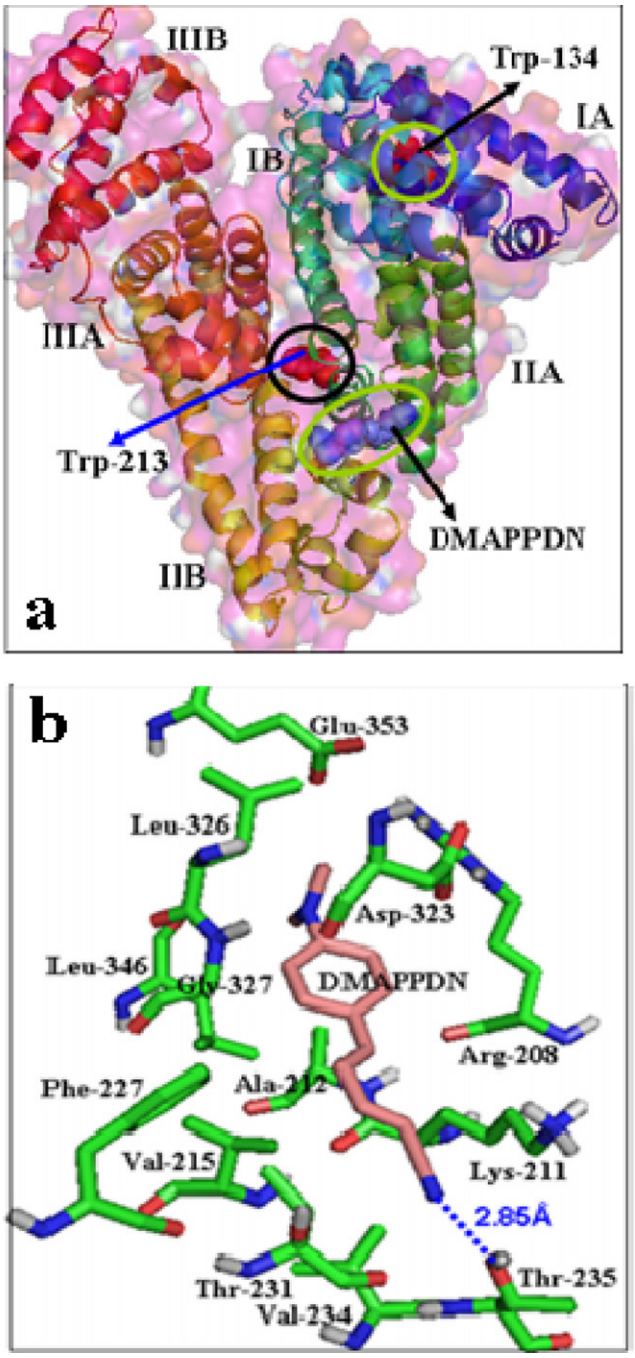

Fig. 6. (a) Minimum energy docking conformation obtained from docking simulation in which each sub domain of BSA, Trp-134, Trp-213, DMAPPDN have been identified. The BSA is presented by ribbon structure with transparent surface where as Tryptophan, DMAPPDN by sphere model. (b) The hydrophobic and hydrophilic amino acid residues surrounding the probe DMAPPDN. One hydrogen bonding interaction between DMAPPDN and Thr-235 with donor acceptor distance 2.85 Å in minimum energy docking pose, presented by stick model using pymol.

Table 1. Docking results also support that the increase in emission intensity of the probe DMAPPDN is mainly due to the complexation and movement of the probe from the more polar hydrophilic buffer environment to the much less polar hydrophobic region.

3.10. Analysis of molecular dynamics trajectories

Protein probe complexation, stability of the complex and rigidity of the protein environment in the presence of probe have

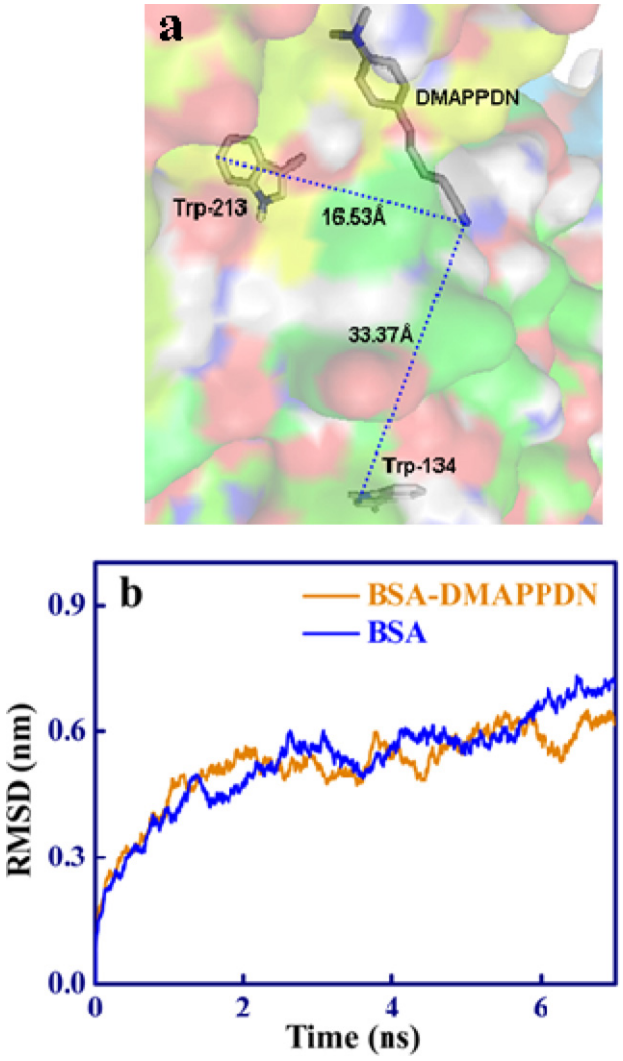

Fig. 7. (a) The distance between Trp-134, Trp-213 and torsion root of DMAPPDN in minimum energy docking pose, presented by stick model using pymol, rest of the protein is shown by transparent surface (b) Plot of root mean square deviation (RMSD) of C—C_α—N backbone vs simulation time scale for solvated BSA and BSA–DMAPPDN after 7 ns molecular dynamics simulations.

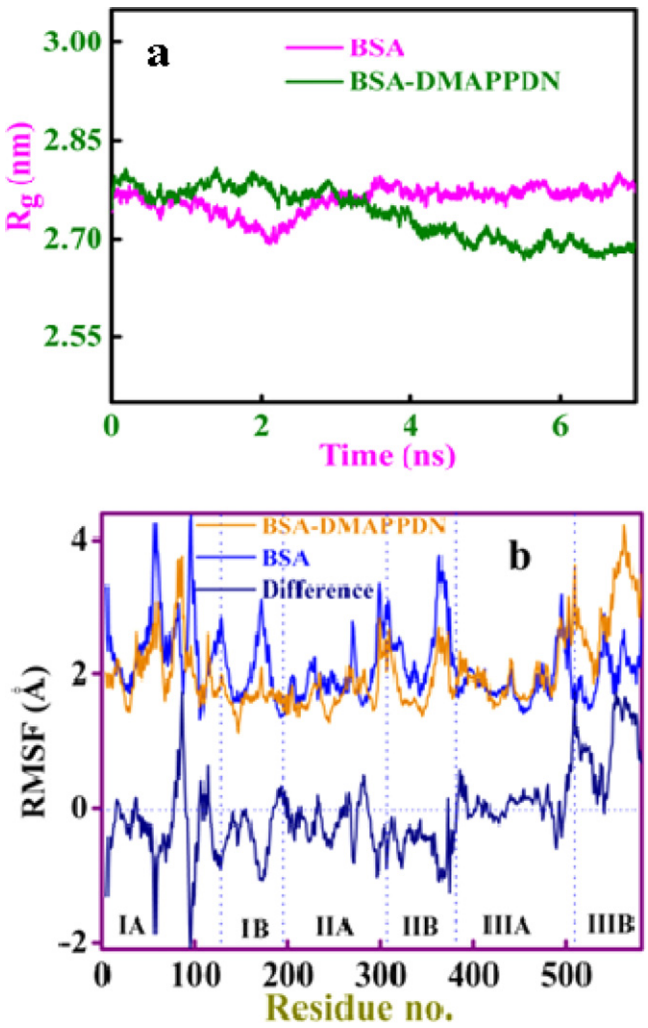

Fig. 8. (a) Plot of radius of gyration (R_g) during 7 ns MD simulation of BSA and BSA–DMAPPDN complex. (b) The root mean square fluctuation (RMSF) values of BSA, its complex with DMAPPDN and the difference between them were plotted against residue numbers for 3–7 ns time scale of the simulation. The residues of different subdomains are separated by vertical dotted lines.

also been discussed from the analysis of MD simulations and all results have been analyzed on the basis of RMSD, RMSF and radius of gyration (R_g) values of the protein with and without binding to the probe in solvated system. The RMSD values of the protein backbone -(C—Cα—N) with and without DMAPPDN were calculated against the simulations times scale (0 to 7 ns.) and the plots are shown in Fig. 7b. From the figure it is seen that for both the free BSA and BSA–DMAPPDN complex the RMSD value steadily increases from 0 to 2 ns, then there is no such increment of RMSD and the systems reaches to equilibrium. After attaining the equilibrium the RMSD values of C—Cα—N backbone for both the BSA and BSA–DMAPPDN complex were calculated for 3 to 7 ns time scale. For BSA, the data point fluctuations are 0.60 ± 0.06 nm where as for the complex are 0.56 ± 0.04 nm [32].

The calculated radius of gyration (R_g) values over the simulation time scale for the native BSA and the BSA–DMAPPDN complex are presented in Fig. 8a. It is seen that the R_g values for native BSA initially fluctuate near 2.76 nm and then reaches to a minimum value of 2.69 nm at 2 ns. After that it increases to 2.77 nm and then remains constant throughout 3–7 ns. On the other hand, for BSA–DMAPPDN complex, starting R_g value of 2.77 nm remains constant up to 3 ns and then decreases to 2.67 nm at 5.5 ns and after that it remains almost constant with slight fluctuations throughout the 7 ns time scale. The constancy of R_g values after 5.5 ns supports attainment of equilibrium. For both the cases, the gyration value starts from 2.76 nm but decreases and fluctuates near 2.77 ± 0.01 nm (4.5–7 ns) for BSA and 2.69 ± 0.01 nm (4.5–7 ns) for BSA–DMAPPDN complex indicating stabilization of the complex with respect to solvated native BSA, which is also true with the conclusions drawn from the CD spectra as described in the supplementary material. Till date there is no report about the crystal structure and also R_g value of BSA, therefore we could not compare the R_g value obtained from simulation with the experimental values. The reported R_g value of HSA (which is 75% homologues and 87% similar in nature with BSA) shown by neutron scattering in aqueous solution was 2.74 ± 0.03 nm [48] which is comparable to our results for BSA. Our simulation is hence pretty accurate in nature. During simulation the little change of R_g value from BSA to BSA–DMAPPDN over simulation time indicates very little conformational changes in the secondary structure of BSA when bound to the DMAPPDN. This observation again supports the CD spectral results as shown in Figure S1 in the supplementary material.

To investigate the local protein mobility we have calculated the time averaged root mean square fluctuation of all the residues over

all time scale and presented in Fig. 8b. As seen in the figure, the drug binding sites sub domain IIA and IIIA are more rigid compared to other sites. Flexibility was also observed at the end of the helix and sub domain where random coiling is present. The rigidity of sub domain IIA increases after complex formation which is obtained from the RMSF difference in Fig. 8b. Other than IIA sub domain the difference of RMSF fluctuates to ±1.3 Å centering to zero. All the other highly fluctuating regions are those, which connect to the helix.

4. Conclusion

In this paper, the binding interaction of the polarity sensitive charge transfer probe DMAPPDN with BSA and denaturation of the protein bound probe by GdnHCl have been studied by spectroscopic techniques in combination with theoretical MD simulations and molecular modeling methods. Red shift of the absorption band (19 nm) and blue shift of emission maxima (78 nm) of the extrinsic fluorophore with manifold enhancement of intensity on the addition of BSA indicate spontaneous complexation ($\Delta G = -5.359\,\text{kcal mol}^{-1}$) with binding constant ($K = 8.821 \pm 0.01 \times 10^3\,\text{M}^{-1}$). Steady rise in anisotropy value and high average lifetime of the probe in the presence of BSA infer tight binding of the probe in the restricted hydrophobic protein interior. FRET and molecular docking studies suggest efficient binding and proper orientation of the probe within the hydrophobic cavity of sub domain IIA. MD simulation studies revealed that BSA and BSA–DMAPPDN complex were stabilized around 3 ns. Chemical denaturation of BSA by GdnHCl has been mapped successfully using the same fluorescence probe. Over all, this charge transfer site specific fluorescent probe can be used to spectroscopically study the biological model protein bovine serum albumin without using any complicated X-ray or NMR analysis.

Acknowledgements

N.G. gratefully acknowledges the financial support received from Department of Science and Technology, India (Project no. SR/S1/PC-26/2008). S.J. and S.D. would like to thank UGC for Fellowship.

Appendix A. Supplementary data

Supplementary data associated with this article can be found, in the online version, at doi:10.1016/j.jphotochem.2011.12.002.

References

[1] E.L. Gelamo, C.H. Silva, H. Imasato, M. Tabak, Interaction of bovine (BSA) and human (HSA) serum albumins with ionic surfactants: spectroscopy and modelling, Biochim. Biophys. Acta 1594 (2002) 84–99.
[2] F.L. Cui, J. Fan, W. Li, Y.C. Fan, Z.D. Hu, Fluorescence spectroscopy studies on 5-aminosalicylic acid and zinc 5-aminosalylicylate interaction with human serum albumin, J. Pharm. Biomed. Anal. 34 (2004) 189–197.
[3] K. Yamasaki, T. Maruyama, U. Kragh-Hansen, M. Otagiri, Characterization of site I on human serum albumin: concept about the structure of a drug binding site, Biochim. Biophys. Acta 1295 (1996) 147–157.
[4] X.M. He, D.C. Carter, Atomic structure and chemistry of human serum albumin, Nature 358 (1992) 209–215.
[5] I. Sjoholm, B. Ekman, A. Kober, I. Ljungstedt-Pahlman, B. Seiving, T. Sjodin, Binding of drugs to human serum albumin: XI. The specificity of three binding sites as studied with albumin immobilized in microparticles, Mol. Pharmacol. 16 (1979) 767–777.
[6] N. Ibrahim, H. Ibrahim, S. Kim, J.-P. Nallet, F.O. Nepveu, Interactions between antimalarial indolone-N-oxide derivatives and human serum albumin, Biomacromolecules 11 (2010) 3341–3351.
[7] H. Benyamini, A. Shulman-Peleg, H.J. Wolfson, B. Belgorodsky, L. Fadeev, M. Gozin, Interaction of C60-fullerene and carboxyfullerene with proteins: docking and binding site alignment, Bioconjugate Chem. 17 (2006) 378–386.
[8] T. Chakraborty, I. Chakraborty, S.P. Moulik, S. Ghosh, Physicochemical and conformational studies on BSA–surfactant interaction in aqueous medium, Langmuir 25 (2009) 3062–3074.
[9] O.K. Abou-Zied, O.I. Al-Shihi, Characterization of subdomain IIA binding site of human serum albumin in its native, unfolded, and refolded states using small molecular probes, J. Am. Chem. Soc. 130 (2008) 10793–10801.
[10] O.K. Abou-Zied, Investigating 2,2′-bipyridine-3,3′-diol as a microenvironment-sensitive probe: its binding to cyclodextrins and human serum albumin, J. Phys. Chem. B 111 (2007) 9879–9885.
[11] D.C. Carter, J.X. Ho, Structure of serum albumin, Adv. Protein Chem. 45 (1994) 153–203.
[12] P.S. Sardar, S. Samanta, S.S. Maity, S. Dasgupta, S. Ghosh, Energy transfer photophysics from serum albumins to sequestered 3-hydroxy-2-naphthoic acid, an excited state intramolecular proton-transfer probe, J. Phys. Chem. B 112 (2008) 3451–3461.
[13] Y. Moriyama, D. Ohta, K. Hachiya, Y. Mitsui, K. Takeda, Fluorescence behavior of tryptophan residues of bovine and human serum albumins in ionic surfactant solutions: a comparative study of the two and one tryptophan(s) of bovine and human albumins, J. Protein Chem. 15 (1996) 265–272.
[14] B.X. Huang, H.-Y. Kim, C. Dass, Probing three-dimensional structure of bovine serum albumin by chemical cross-linking and mass spectrometry, J. Am. Soc. Mass Spectrom. 15 (2004) 1237–1247.
[15] D.C. Carter, X.M. He, Structure of human serum albumin, Science 249 (1990) 302–303.
[16] S. Ghosh, N. Guchhait, Chemically induced unfolding of bovine serum albumin by urea and sodium dodecyl sulfate: a spectral study with the polarity-sensitive charge-transfer fluorescent probe (E)-3-(4-methylaminophenyl)acrylic acid methyl ester, Chem. Phys. Chem. 10 (2009) 1664–1671.
[17] B. Ahmad, M.Z. Ahmed, S.K. Haq, R.H. Khan, Guanidine hydrochloride denaturation of human serum albumin originates by local unfolding of some stable loops in domain III, Biochimi. Biophys. Acta: Proteins Proteom. 1750 (2005) 93–102.
[18] S. Ghosh, S. Jana, D. Nath, N. Guchhait, Fluorescent probing of protein bovine serum albumin stability and denaturation using polarity sensitive spectral response of a charge transfer probe, J. Fluoresc. 21 (2011) 365–374.
[19] J. Li, X. Zhu, C. Yang, R. Shi, Characterization of the binding of angiotensin II receptor blockers to human serum albumin using docking and molecular dynamics simulation, J. Mol. Model. 16 (2010) 789–798.
[20] S. Neelam, M. Gokara, B. Sudhamalla, D.G. Amooru, R. Subramanyam, Interaction studies of coumaroyltyramine with human serum albumin and its biological importance, J. Phys. Chem. B 114 (2010) 3005–3012.
[21] F. Chiappori, P. D'Ursi, I. Merelli, L. Milanesi, E. Rovida, In silico saturation mutagenesis and docking screening for the analysis of protein–ligand interaction: the endothelial protein C receptor case study, BMC Bioinf. 10 (2009) S3.
[22] O. Deeb, M.C. Rosales-Hernandez, C. Gomez-Castro, R. Garduno-Juarez, J. Correa-Basurto, Exploration of human serum albumin binding sites by docking and molecular dynamics flexible ligand–protein interactions, Biopolymers 93 (2010) 161–170.
[23] B. Sudhamalla, M. Gokara, N. Ahalawat, D.G. Amooru, R. Subramanyam, Molecular dynamics simulation and binding studies of β-sitosterol with human serum albumin and its biological relevance, J. Phys. Chem. B 114 (2010) 9054–9062.
[24] S. Jana, S. Dalapati, S. Ghosh, S. Kar, N. Guchhait, Excited state charge transfer reaction with dual emission from 5-(4-dimethylamino-phenyl)-penta-2,4-dienenitrile: spectral measurement and theoretical density functional theory calculation, J. Mol. Struct. 998 (2011) 136–143.
[25] S. Bhattacharya, T.K. Pradhan, A. De, S.R. Chaudhury, A.K. De, T. Ganguly, Photophysical processes involved within the anisole–thioindoxyl dyad system, J. Phys. Chem. A 110 (2006) 5665–5673.
[26] G.M. Morris, D.S. Goodsell, R.S. Halliday, R. Huey, W.E. Hart, R.K. Belew, A.J. Olson, Automated docking using a Lamarckian genetic algorithm and an empirical binding free energy function, J. Comput. Chem. 19 (1998) 1639–1662.
[27] J.C. Phillips, R. Braun, W. Wang, J. Gumbart, E. Tajkhorshid, E. Villa, C. Chipot, R.D. Skeel, L. Kalé, K. Schulten, Scalable molecular dynamics with NAMD, J. Comput. Chem. 26 (2005) 1781–1802.
[28] A.D. MacKerell, D. Bashford, Bellott, R.L. Dunbrack, J.D. Evanseck, M.J. Field, S. Fischer, J. Gao, H. Guo, S. Ha, D. Joseph-McCarthy, L. Kuchnir, K. Kuczera, F.T.K. Lau, C. Mattos, S. Michnick, T. Ngo, D.T. Nguyen, B. Prodhom, W.E. Reiher, B. Roux, M. Schlenkrich, J.C. Smith, R. Stote, J. Straub, M. Watanabe, J. Wiórkiewicz-Kuczera, D. Yin, M. Karplus, All-atom empirical potential for molecular modeling and dynamics studies of proteins, J. Phys. Chem. B 102 (1998) 3586–3616.
[29] A. Pedretti, L. Villa, G. Vistoli, VEGA—an open platform to develop chemo-bioinformatics applications, using plug-in architecture and script programming, J. Comput. Aid. Mol. Des. 18 (2004) 167–173.
[30] W. Humphrey, A. Dalke, K. Schulten, VMD: visual molecular dynamics, J. Mol. Graph. 14 (1996) 33–38, 27–38.
[31] P.F. Batcho, D.A. Case, T. Schlick, Optimized particle-mesh Ewald/multiple-time step integration for molecular dynamics simulations, J. Chem. Phys. 115 (2001) 4003–4018.
[32] E. Jardón-Valadez, A. Ulloa-Aguirre, A.N. Piñeiro, Modeling and molecular dynamics simulation of the human gonadotropin-releasing hormone receptor in a lipid bilayer, J. Phys. Chem. B 112 (2008) 10704–10713.
[33] R.B. Singh, S. Mahanta, A. Bagchi, N. Guchhait, Interaction of human serum albumin with charge transfer probe ethyl ester of N,N-dimethylamino naphthyl acrylic acid: an extrinsic fluorescence probe for studying protein microenvironment, Photochem. Photobiol. Sci. 8 (2009) 101–110.

[34] H.A. Benesi, J.H. Hildebrand, A spectrophotometric investigation of the interaction of iodine with aromatic hydrocarbons, J. Am. Chem. Soc. 71 (1949) 2703–2707.
[35] S. Mahanta, R.B. Singh, N. Guchhait, Study of protein–probe interaction and protective action of surfactant sodium dodecyl sulphate in urea-denatured HSA using charge transfer fluorescence probe methyl ester of N,N-dimethylamino naphthyl acrylic acid, J. Fluoresc. 19 (2009) 291–302.
[36] D. Sarkar, A. Mahata, P. Das, A. Girigoswami, D. Ghosh, N. Chattopadhyay, Deciphering the perturbation of serum albumins by a ketocyanine dye: a spectroscopic approach, J. Photochem. Photobiol. B 96 (2009) 136–143.
[37] S. Haldar, A. Chattopadhyay, Dipolar relaxation within the protein matrix of the green fluorescent protein: a red edge excitation shift study, J. Phys. Chem. B 111 (2007) 14436–14439.
[38] A. Chattopadhyay, S. Mukherjee, Red edge excitation shift of a deeply embedded membrane probe: implications in water penetration in the bilayer, J. Phys. Chem. B 103 (1999) 8180–8185.
[39] A. Mallick, B. Haldar, N. Chattopadhyay, Spectroscopic investigation on the interaction of ICT probe 3-acetyl-4-oxo-6,7-dihydro-12H indolo-[2,3-a] quinolizine with serum albumins, J. Phys. Chem. B 109 (2005) 14683–14690.
[40] D.M. Davis, D.J.S. Birch, Extrinsic fluorescence probe study of human serum albumin using Nile red, J. Fluoresc. 6 (1996) 23–32.
[41] F.-Y. Wu, Z.-J. Ji, Y.-M. Wu, X.-F. Wan, Interaction of ICT receptor with serum albumins in aqueous buffer, Chem. Phys. Lett. 424 (2006) 387–393.
[42] A. Banerjee, K. Basu, P.K. Sengupta, Interaction of 7-hydroxyflavone with human serum albumin: a spectroscopic study, J. Photochem. Photobiol., B 90 (2008) 33–40.
[43] S. Jana, S. Ghosh, S. Dalapati, S. Kar, N. Guchhait, Photoinduced intramolecular charge transfer phenomena in 5-(4-dimethylamino-phenyl)-penta-2,4-dienoic acid, Spectrochim. Acta Part A 78 (2011) 463–468.
[44] Z.R. Grabowski, K. Rotkiewicz, W. Rettig, Structural changes accompanying intramolecular electron transfer: focus on twisted intramolecular charge-transfer states and structures, Chem. Rev. 103 (2003) 3899–4032.
[45] R. Misra, A. Mandal, M. Mukhopadhyay, D.K. Maity, S.P. Bhattacharyya, Spectral signatures of intramolecular charge transfer process in beta-enaminones: a combined experimental and theoretical analysis, J. Phys. Chem. B 113 (2009) 10779–10791.
[46] S.S. Krishnakumar, D. Panda, Spatial relationship between the prodan site, Trp-214, and Cys-34 residues in human serum albumin and loss of structure through incremental unfolding, Biochemistry 41 (2002) 7443–7452.
[47] S. Muzammil, Y. Kumar, S. Tayyab, Anion-induced stabilization of human serum albumin prevents the formation of intermediate during urea denaturation, Proteins 40 (2000) 29–38.
[48] M.A. Kiselev, Y.A. Gryzunov, G.E. Dobretsov, M.N. Komarova, The size of human serum albumin molecules in solution, Biofizika 46 (2001) 423–427.